Received: 25 April 2022 | Revised: 16 August 2022 | Accepted: 1 September 2022

DOI: 10.1002/jat.4391

RESEARCH ARTICLE

Journal of Applied Toxicology WILEY

Lanthanum nitrate inhibits adipogenesis in 3T3-L1 preadipocytes with a disorder of mitotic clonal expansion process

Linglu Xu | Qianqian Xiao | Chenping Kang | Xuetao Wei | Weidong Hao

Department of Toxicology, School of Public Health, Peking University, Beijing Key Laboratory of Toxicological Research and Risk Assessment for Food Safety, Beijing 100191, China

Correspondence
Weidong Hao, Department of Toxicology, School of Public Health, Peking University, Beijing Key Laboratory of Toxicological Research and Risk Assessment for Food Safety, Beijing 100191, China.
Email: whao@bjmu.edu.cn

Funding information
National Key Research and Development Program of China, Grant/Award Number: 2017YFC1600203

Abstract

Lanthanum (La) as a rare earth element is widely used in agriculture, industry, and medicine. It has been suggested in several studies that La might influence glycolipid metabolism in vivo. In this study, we used 3T3-L1 preadipocytes as in vitro cell model to elucidate the effects of $La(NO_3)_3$ on adipogenesis and the underlying mechanisms. The results showed that $La(NO_3)_3$ could inhibit the adipogenic differentiation of 3T3-L1 preadipocytes, which showed a decrease in lipid accumulation and the down-regulation of specific adipogenic transcription factors. $La(NO_3)_3$ exerted its inhibitory effect mainly at the early differentiation stage. Furthermore, $La(NO_3)_3$ influenced the S-phase entry and cell cycle process during the mitotic clonal expansion and regulated the phosphorylation of signal transducer and activator of transcription 3 (STAT3) and expressions of the proteins in phosphatidylinositol 3-kinase (PI3K)/Akt pathway at the early stage of differentiation. Besides, $La(NO_3)_3$ upregulated the expressions of *wnt10b* mRNA and β-catenin protein and promoted the nucleus translocation of β-catenin. Additionally, we found that $La(NO_3)_3$ could promote the growth of 3T3-L1 preadipocytes both with and without MDI (3-isobutyl-1-methylxanthine [IBMX], dexamethasone [Dex], and insulin) stimulation. Collectively, these results indicated that $La(NO_3)_3$ could inhibit adipogenesis in 3T3-L1 preadipocytes and influence cell proliferation.

KEYWORDS
3T3-L1 preadipocytes, adipogenesis, lanthanum nitrate, mitotic clonal expansion, wnt/β-catenin signaling pathway

1 | INTRODUCTION

Rare earth elements (REEs) include 15 lanthanides, plus the transition metals scandium and yttrium, and play important roles in agriculture, industry, military, and medicine due to their physical and chemical properties. The widespread use of REEs also leads to pollution of the environment, increases the potential for human exposure, and raises concerns about their adverse effects (Grosjean et al., 2019). As a representative of the light REEs, lanthanum (La) and its compounds are widely used in various applications and tend to accumulate in the organs of the body, such as the liver and brain, so it is necessary to figure out the health effects of their accumulation in the human body (Han et al., 2021). Several studies have suggested that La and its compounds might regulate lipid metabolism and adipogenesis. The results of animal experiments showed that lanthanide exposure caused some liver tissue lesions and functional impairment, including hepatic steatosis and inflammatory cell infiltration (Chen et al., 2003; Cheng et al., 2014). Also, a recent in vivo experiment found that low-dose lanthanum nitrate ($La(NO_3)_3$) exposure could modulate lipid metabolism and ameliorate atherosclerosis induced by high-fat diet in

ApoE$^{-/-}$ mice (Li et al., 2021). In vitro experiments showed that lanthanide chlorides inhibited adipogenesis in 3T3-L1 preadipocytes and La exposure inhibited the expression of adipogenic genes in mouse mesenchymal stromal cells (MSCs) and primary mouse osteoblasts (He et al., 2006; Hou et al., 2013; Liu et al., 2015; Zhang et al., 2012). It highlighted the health hazard caused by La focusing on adipogenesis and in vivo lipid metabolism and the importance of exploring the possible mechanisms of its effects.

Adipose tissue is a highly heterogeneous and metabolically active organ containing various cell types including adipocytes, endothelial cells, preadipocytes, and macrophages (Sarjeant & Stephens, 2012). In addition to the classical functions of energy storage, body insulation, and mechanical protection, adipose tissue also has some biological functions as an important endocrine organ of the body. Adipose tissue can synthesize and secrete various adipokines, which act through paracrine, autocrine, and endocrine (Galic et al., 2010; McGown et al., 2014), and regulate many physiological and pathophysiological processes such as lipid and glucose metabolism, blood flow regulation, insulin sensitivity, and immune system function (Poulos et al., 2010). Under the sustained imbalance between energy intake and expenditure, adipose tissue will expand through the increase in adipocyte progenitor differentiation or the enlargement of adipocyte cell size, progressively resulting in the development of obesity, adipose tissue dysfunction, and metabolic diseases (Kawai et al., 2021). It was also proved that conditions of adipose tissue deficiency or lipodystrophy were also associated with insulin resistance, glucose intolerance, inflammation, and other metabolic syndromes in humans and rodents (Capeau et al., 2005; Leow et al., 2003). Also, the homeostatic balance of glucose and lipid metabolism is important for the body to cope with changes in the internal and external environment. In conclusion, as an endocrine organ, excess or deficiency of adipose tissue might have adverse metabolic consequences for the organisms and need to be taken into account.

Adipogenesis is a complex process that involves the commitment from MSCs to preadipocytes and the differentiation to the mature adipocytes (Ali et al., 2013; Lefterova & Lazar, 2009). After the appropriate hormonal stimulation, post-confluent preadipocytes firstly undergo mitotic clonal expansion (MCE), during which the cells arrested in the G1 phase re-enter the cell cycle and begin one or two rounds of replications. Many cell cycle-related proteins and pathways are involved in the MCE process, including CDK2, cyclin D1, retinoblastoma (Rb), and phosphatidylinositol 3-kinase (PI3K)/Akt signaling pathway. The cells then exit the cell cycle for the subsequent early and terminal differentiation and acquire the adipocyte phenotype. A variety of transcription factors are involved in regulating the differentiation process, among which the peroxide proliferative activation receptor (PPAR) and CCAAT/enhancer-binding protein (C/EBP) family exert critical functions in the differentiation. When the cells cross the G1/S checkpoint, C/EBPβ gets DNA-binding activity and subsequently induces the expressions of C/EBPα and PPARγ, which collaborate with each other to transcriptionally activate downstream adipocyte-specific genes expressions, including leptin (lep) and lipoprotein lipase (lpl) (Chang & Kim, 2019). Besides, PPARγ has two protein isoforms, among which PPARγ2 is abundantly expressed in adipocytes and PPARγ1 can be found in many tissues. There are also plenty of signaling pathways that participate in adipogenic differentiation. Studies have shown that the canonical wnt pathway could affect adipogenesis as an important negative regulator, and β-catenin served as an integral mediator in the pathway. With the signal of wnt10b, stabilized β-catenin accumulates in the cytoplasm and then translocates to the nucleus, where it binds to the lymphoid enhancer factor/T-cell factor transcription factors to activate wnt response genes, such as cyclin D1, and inhibit adipogenesis by blocking the expressions of C/EBPα and PPARγ (Christodoulides et al., 2009; Longo et al., 2004).

The 3T3-L1 preadipocyte is one of the most frequently used models for studying adipogenesis in vitro and can be differentiated into mature adipocytes under the proper stimulations. Although it was suggested that $La(NO_3)_3$ might have a potential effect on the glycolipid metabolism in vivo and adipogenic differentiation in vitro, the underlying mechanisms still remained unknown. Herein, in this study, we studied the effect of $La(NO_3)_3$ on adipogenesis in vitro and explored its mechanisms using 3T3-L1 preadipocytes.

2 | MATERIALS AND METHODS

2.1 | Chemicals and reagents

Lanthanum nitrate ($La(NO_3)_3{\cdot}6H_2O$, CAS: 10277-43-7) was purchased from Sigma-Aldrich (St. Louis, MO, USA) and dissolved in distilled water. Dulbecco's modified Eagle's medium (DMEM, high glucose), heat-inactivated bovine serum (HIBS), and penicillin–streptomycin were purchased from Thermo Fisher Scientific (Waltham, MA, USA). Fetal bovine serum was purchased from Gemini Bio-Products (West Sacramento, CA, USA). Human insulin, dexamethasone (Dex), 3-isobutyl-1-methylxanthine (IBMX), 0.5% Oil Red O solution, and paraformaldehyde were purchased from MilliporeSigma (St. Louis, MO, USA).

2.2 | Cell culture, differentiation, and treatment

Mouse 3T3-L1 preadipocytes (CL-173) were purchased from American Type Culture Collection (ATCC, Manassas, VA, USA) and maintained at subconfluence in growth medium (basic DMEM containing 10% HIBS, 1.5 g/L $NaHCO_3$, 100 U/ml penicillin, 100 μg/ml streptomycin, and 2 mM L-glutamine) at 37°C and 5% CO_2 under humidified atmosphere. For differentiation, when reaching 70–80% confluence, the cells were seeded at 5×10^4/ml in six-well plates. Two days after confluence (designated as Day 0), the cells were subjected to adipocyte differentiation for 8 days (Days 0–8). On Days 0–2, the medium was replaced with the differentiation medium I (basic DMEM containing 10% fetal bovine serum [FBS], 1 μg/ml insulin, 250 nM Dex, and 500 μM IBMX). On Days 2–4, the medium was replaced with medium II (basic DMEM containing 10% FBS and 1 μg/ml insulin). Subsequently, the cells were maintained in medium III (basic DMEM containing 10% FBS) up to Day 8, and the medium was changed every 2 days.

The cells were treated with $La(NO_3)_3$ when the cells were not confluent or during different differentiation stages for specific aims. $La(NO_3)_3$ was added to the medium to reach the final concentrations of 1, 5, 10, and 20 μM.

2.3 | Measurement of cytotoxicity with CCK8

3T3-L1 preadipocytes were seeded at 5×10^4/ml in 100 μl of the medium into 96-well plates. After 24 h, the cells were treated with different concentrations of $La(NO_3)_3$ for 48 h. Then, 10 μl of the Cell Counting Kit-8 (CCK8) solution was added to each well, and the cells were incubated at 37°C for 1 h. The absorbance was measured at 450 nm. The cell viability was calculated as a percentage relative to the corresponding control.

2.4 | Living cell count with trypan blue staining

3T3-L1 preadipocytes were seeded at 5×10^4/ml in six-well plates and treated with $La(NO_3)_3$ in the growth medium. After 12, 24, and 48 h, the cells were washed with phosphate-buffered saline (PBS), treated with 0.25% trypsin–0.53 mM EDTA, and centrifuged at 800 rpm for 5 min. The cells were suspended in PBS, stained with 0.4% trypan blue dye, and counted immediately using a hemocytometer.

2.5 | Oil Red O staining

3T3-L1 preadipocytes seeded at 5×10^4/ml in six-well plates were differentiated as described in Section 2.2 and treated with different concentrations of $La(NO_3)_3$. After 8 days, the cells were washed twice with PBS, fixed with 4% paraformaldehyde for 30 min at room temperature, and then washed twice with PBS. The lipid droplets were stained with filtered Oil Red O solution for 1 h at room temperature. The stained cells were then washed with distilled water four times and visualized by microscopy.

2.6 | Measurement of triglyceride (TG) content

3T3-L1 preadipocytes seeded at 5×10^4/ml in six-well plates were differentiated and treated with different concentrations of $La(NO_3)_3$. After 8 days, the cells were harvested and cellular TG contents were quantified using a TG assay kit (Elabscience Biotechnology Co., Ltd, Wuhan, China) according to the manufacturer's instructions. TG contents were normalized with the respective protein concentration.

2.7 | RNA extraction and real-time fluorescent quantitative polymerase chain reaction (RT-qPCR)

Total RNA was extracted using the TransZol Up Plus Kit (TransGen Biotech, Beijing, China). RNA was then subjected to reverse transcription using the TransScript One-Step gDNA Removal and cDNA Synthesis SuperMix Kit (TransGen Biotech). Gene expression was detected using the TransStart Top Green qPCR SuperMix Kit (TransGen Biotech) and analyzed by iQ5 (Bio-Rad Laboratories, California, USA). The sequences of all primers used are shown in Table 1 (AuGCT, Beijing, China). Of these, β-actin was used as a reference gene for normalization, and the relative expression of mRNA was measured by the $2^{-\Delta\Delta CT}$ method.

2.8 | Western blot analysis

The cells were harvested after differentiation, washed twice with PBS, and lysed using radioimmunoprecipitation assay (RIPA) lysis buffer (Beyotime Biotechnology, Shanghai, China) containing protease and phosphatase inhibitor. The cytoplasmic protein and nucleoprotein were extracted using Nuclear and Cytoplasmic Protein Extraction Kit (Beyotime) according to the manufacturer's instructions. Protein amounts were measured using a Pierce BCA Protein Assay Kit (Thermo Fisher Scientific); 30 μg protein was loaded on 10% sodium dodecyl sulfate (SDS)–polyacrylamide gel electrophoresis (PAGE) gels after being denatured in SDS sample buffer. The proteins were then transferred to nitrocellulose (NC) membranes (0.45 μm, Millipore, Ireland). The membranes were blocked in 5% (w/v) skim milk for 2 h at room temperature, incubated with primary antibodies (Table 2) overnight at 4°C, and then incubated with the secondary antibody for 2 h at room temperature. The protein bands were visualized by ECL fluid (Beijing Biodragon Immunotechnologies, Beijing, China) and analyzed using a chemiluminescence analyzer (Mini HD9, UVITEC, Cambridge, UK).

2.9 | Fluorescence-activated cell sorting (FACS) analysis

Cell cycle progression was assessed by FACS. Cells were harvested after differentiation at indicated time points, washed with PBS,

TABLE 1 qPCR primer sequences

Gene	Forward (5′–3′)	Reverse (5′–3′)
Lep	CATTTCACACACGCAGTCGGTATCC	GGGAAGGCAGGCTGGTGAGGAC
Lpl	TCTCCTGATGACGCTGATTTTG	TCTCTTGGCTCTGACCTTGTTG
Wnt10b	GACGCCAGGTGGTAACGGAAAAC	TGCTCAGCCGCTCCCTCAGTG
β-Actin	GGCTGTATTCCCCTCCATCG	CCAGTTGGTAACAATGCCATGT

trypsinized, and centrifuged at 800 rpm for 5 min. The pellets were washed with PBS twice and then fixed in 70% ethanol overnight at 4°C. Then, cells were rinsed twice with PBS and incubated with PI solution (Beijing Dingguo Changsheng Biotechnology, Beijing, China) containing 10 μg/ml RNase A for 30 min. FACS analysis was performed using a CytoFLEX flow cytometer (Beckman Coulter, Brea, USA), and DNA content was equivalent to the fluorescent of incorporated PI. The percentages of cells in G0/G1, S, and G2/M phases were analyzed by CytExpert software (Beckman Coulter).

2.10 | Immunofluorescence

The 3T3-L1 preadipocytes seeded on the coverslips inside six-well plates were differentiated and treated with 20 μM $La(NO_3)_3$. The cells were fixed with 4% paraformaldehyde at room temperature, washed with PBS three times, and permeabilized with 0.3% Triton X-100 for 30 min. Afterward, the cells were blocked with Immunol Staining Blocking Buffer (Beyotime Biotechnology) for 1 h and incubated overnight with primary antibodies at 4°C. The cells were then rinsed with PBS and treated with Alexa Fluor 488 anti-rabbit secondary antibodies (1:500) (Beyotime Biotechnology) for 1 h and washed. DAPI (Beyotime Biotechnology) was added to stain nuclear for 5 min. Stained cells were viewed with a Nikon A1 confocal microscope using NIS-Elements (Tokyo, Japan).

2.11 | Statistical analysis

All experiments were repeated three times. The results were presented as the mean ± SD. Data were analyzed using IBM SPSS Version 26.0 (SPSS Inc., Chicago, IL, USA). The significance of the differences between the control and treatment groups was evaluated by one-way analysis of variance (ANOVA) followed by Dunnett's multiple comparison test. $p < 0.05$ was statistically significant.

TABLE 2 Primary antibodies for Western blot analysis

Name	Animal	Dilution	Brand	Product number
PPARγ (81B8)	Rabbit	1:1000	CST	2443
C/EBPα (D56F10)	Rabbit	1:1000	CST	8178
pSTAT3 (Tyr705) (D3A7)	Rabbit	1:1000	CST	9145
STAT3 (124H6)	Rabbit	1:1000	CST	9139
C/EBPβ (E299)	Rabbit	1:1000	Abcam	ab32358
β-Catenin	Rabbit	1:1000	Absin	abs121277
CDK2 (78B2)	Rabbit	1:1000	CST	2546
Akt	Rabbit	1:1000	Abmart	T55561
pAkt (Thr308)	Rabbit	1:1000	Abmart	T40068
pPI3K (Tyr467/199)	Rabbit	1:1000	Abmart	T40116
PI3K	Rabbit	1:1000	Abmart	T40115
Cyclin D1	Rabbit	1:500	Beyotime	AF1183
Histone H3 (D1H2)	Rabbit	1:1000	CST	4499
β-Actin (D6A8)	Rabbit	1:1000	CST	8457

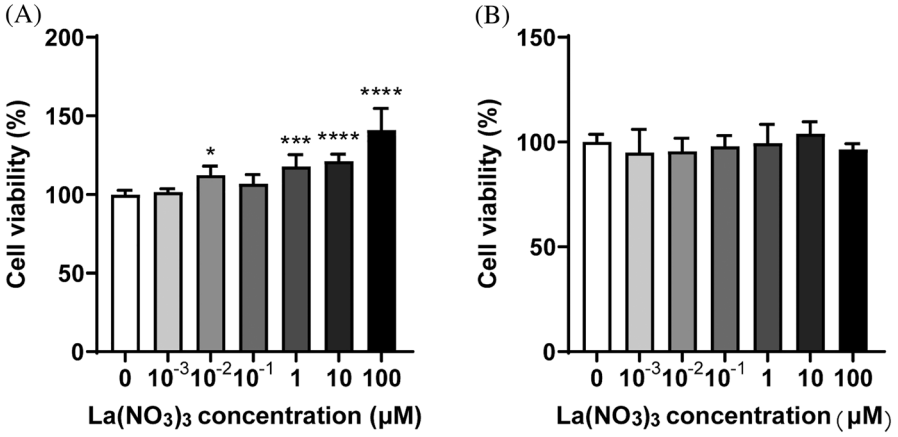

FIGURE 1 $La(NO_3)_3$ promoted the growth of 3T3-L1 preadipocytes. The cells were treated with $La(NO_3)_3$ in the presence or absence of the differentiation medium. The effects of $La(NO_3)_3$ on cell viability of (A) preadipocytes and (B) differentiated preadipocytes were evaluated with CCK8 assay. The cell viability was calculated by normalizing the absorbance to the control group. The data are presented as the mean ± SD. $n = 3$. $^{*}p < 0.05$, $^{***}p < 0.001$, and $^{****}p < 0.0001$ compared to the control group.

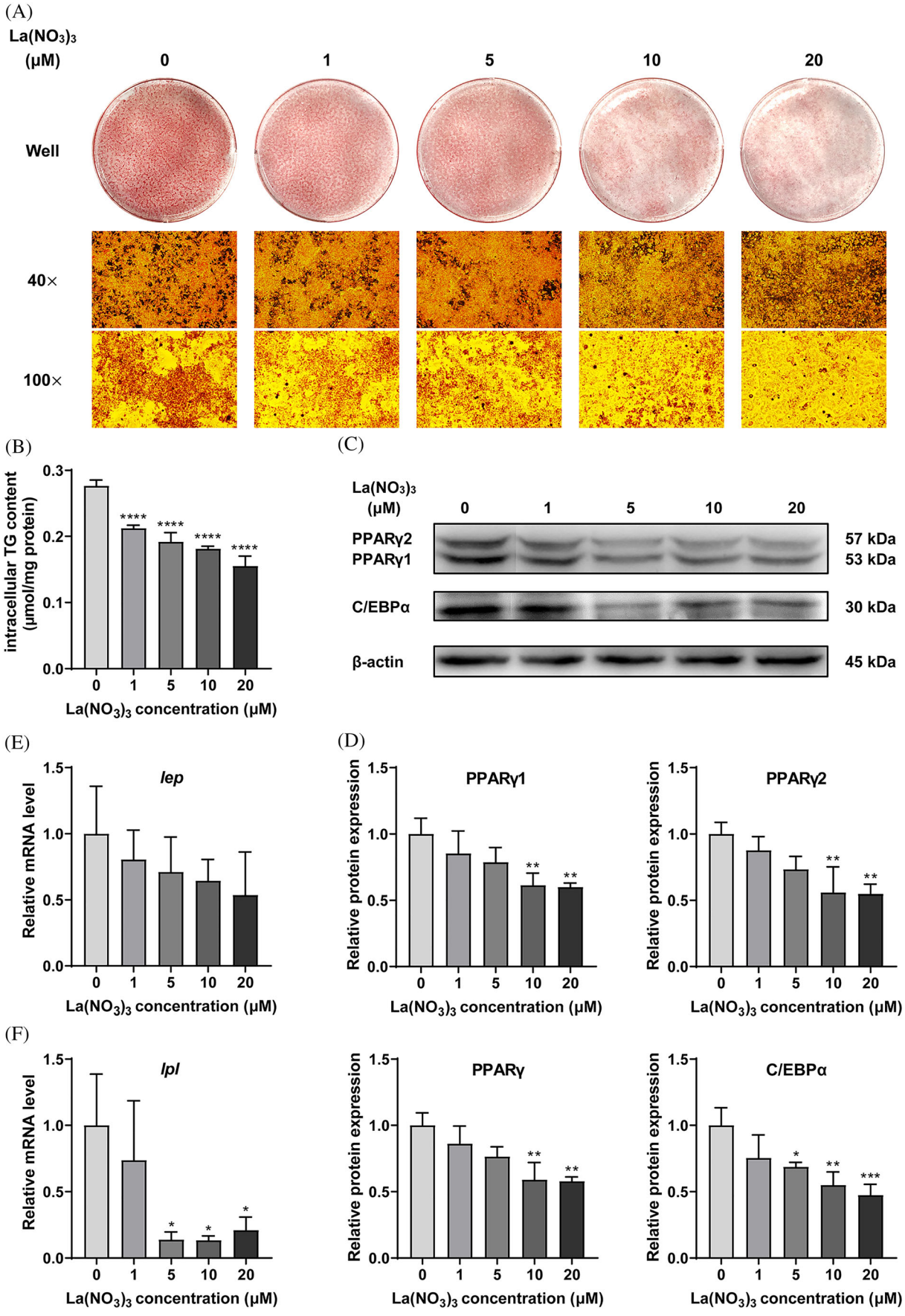

FIGURE 2 Legend on next page.

FIGURE 2 $La(NO_3)_3$ inhibited adipogenic differentiation of 3T3-L1 preadipocytes. The cells were induced by MDI medium and treated with $La(NO_3)_3$ in different concentrations. On Day 8, the cells were stained with Oil Red O and photographed, the intracellular TG contents were quantified using assay kits, and the protein expression levels of PPARγ1/2 and C/EBPα were measured. (A) The images of Oil Red O staining of the cells treated on Days 0–8. The first row shows images of a single well of a six-well plate. The second row displays photographs taken under an inverted microscope (40×). The third row displays photographs taken under an inverted microscope (100×). (B) The intracellular TG contents in the cells treated on Days 0–8. The results were standardized using protein concentrations. (C) The protein expression levels of PPARγ1/2 and C/EBPα in the cells treated on Days 0–8. β-Actin was used as the loading protein. The protein bands were quantified using ImageJ software. (D) Relative protein expression levels of PPARγ1/2 and C/EBPα. (E) The mRNA expression levels of *lep*. (F) The mRNA expression levels of *lpl*. The relative mRNA expression levels were calculated using $2^{-\Delta\Delta Ct}$ method. The data are presented as the mean ± SD. $n = 3$. $^{*}p < 0.05$, $^{**}p < 0.01$, $^{***}p < 0.001$, and $^{****}p < 0.0001$ compared to the control group.

3 | RESULTS

3.1 | $La(NO_3)_3$ promoted the growth of 3T3-L1 preadipocytes

The cytotoxic effects were evaluated by the CCK8 assay. The results showed that the treatment of $La(NO_3)_3$ for 48 h had no obvious toxicity up to 100 μM and had a certain role in promoting cell growth on the preadipocytes at more than 1 μM (Figure 1A). The cell viability was also measured in the cells after MDI induction for 8 days, and no cytotoxicity was observed under the treatment (Figure 1B). Therefore, 1, 5, 10, and 20 μM of $La(NO_3)_3$ were applied in the following experiments.

3.2 | $La(NO_3)_3$ inhibited adipogenic differentiation of 3T3-L1 preadipocytes

To evaluate the effects of $La(NO_3)_3$ on adipogenesis in 3T3-L1 preadipocytes, the lipid accumulation and adipogenesis-associated biomarkers were detected on Day 8 when the cells were fully differentiated. As shown in Figure 2A, lipid droplets with Oil Red O staining were potently induced in the control group, which indicated effective adipocyte differentiation. And $La(NO_3)_3$ significantly suppressed lipid accumulation in a dose-dependent manner. Consistently, compared to the control group, the intracellular TG contents were dose-dependently decreased in the cells treated with $La(NO_3)_3$ (Figure 2B).

Adipogenesis is modulated by various transcription factors, among which C/EBPs and PPARγ play key roles in the complex transcriptional cascade during differentiation. Therefore, we examined the expression of PPARγ and C/EBPα to verify the inhibitory effect of $La(NO_3)_3$ on the differentiation. As shown in Figure 2C,D, compared to the control, the expressions of both transcription factors PPARγ and C/EBPα were significantly reduced in the cells treated with 10 and 20 μM $La(NO_3)_3$. The mRNA expression levels of adipocyte-specific genes *lep* and *lpl* were detected. The results showed the expression of *lpl* was downregulated in the cells treated above 5 μM $La(NO_3)_3$, and although there was no statistical difference, a slight decrease in the expression of *lep* was also observed (Figure 2E,F). These results demonstrated that $La(NO_3)_3$ inhibited the adipogenesis process of 3T3-L1 preadipocytes.

3.3 | $La(NO_3)_3$ blocked the adipogenesis at the early stage of differentiation

It is well known that the process of adipocyte differentiation from preadipocytes occurs in four main stages, including growth arrest after confluence (Days −2 to 0), MCE (Days 0–2), early differentiation (Days 2–4), and terminal differentiation (Days 4–8). In order to find the critical stage of the inhibitory effect, 3T3-L1 preadipocytes were treated with 20 μM $La(NO_3)_3$ at different times during the differentiation process (Figure 3A). The results of Oil Red O staining showed that the inhibitory effect of $La(NO_3)_3$ on the lipid accumulation was strongest in the cells treated on Days 0–2, which was comparable to that in the cells exposed to $La(NO_3)_3$ on Days 0–8 (Figure 3B). Treatment with $La(NO_3)_3$ on Days 4–8 reduced the intracellular TG content moderately compared to the control cells, and the TG content in the cells treated on Days 2–4 was similar to the control (Figure 3B). The expression levels of PPARγ2 and C/EBPα reduced in the cells exposed to $La(NO_3)_3$ on Days 0–2 and 0–8, and the expression levels in the cells treated on Days 2–4 and 4–8 were similar to the control (Figure 3C,D). These results indicated that $La(NO_3)_3$ might exert the inhibitory effect mainly during the early stage of differentiation.

3.4 | The effects of $La(NO_3)_3$ on cell proliferation and cell cycle progression during MCE

In the early phase of adipogenic differentiation, growth-arrested 3T3-L1 preadipocytes re-enter the cell cycle and undergo the MCE process, which is a prerequisite for the differentiation of 3T3-L1 preadipocytes, to continue the following differentiation stages. Therefore, we investigated the effect of $La(NO_3)_3$ on MCE, focusing on the MDI-stimulated cell proliferation and cell cycle. The results from the trypan blue assay revealed that $La(NO_3)_3$ treatment for 48 h caused an increase in cell proliferation when the cells were in the MCE phase (Figure 4A).

The distributions of the cell cycle at different time points after the $La(NO_3)_3$ treatment were shown in Figure 4B,C, respectively. Before the differentiation, the post-confluent cells mainly remained at the G0/G1 phase, and then the cells re-entered the cell cycle after the MDI induction. The differentiating cells entered the S phase with a peak at about 16 h. The proportion of the S phase was increased obviously in the cells treated with $La(NO_3)_3$ (Table 3), which indicated that $La(NO_3)_3$ might promote a cell cycle transition from the G0/G1

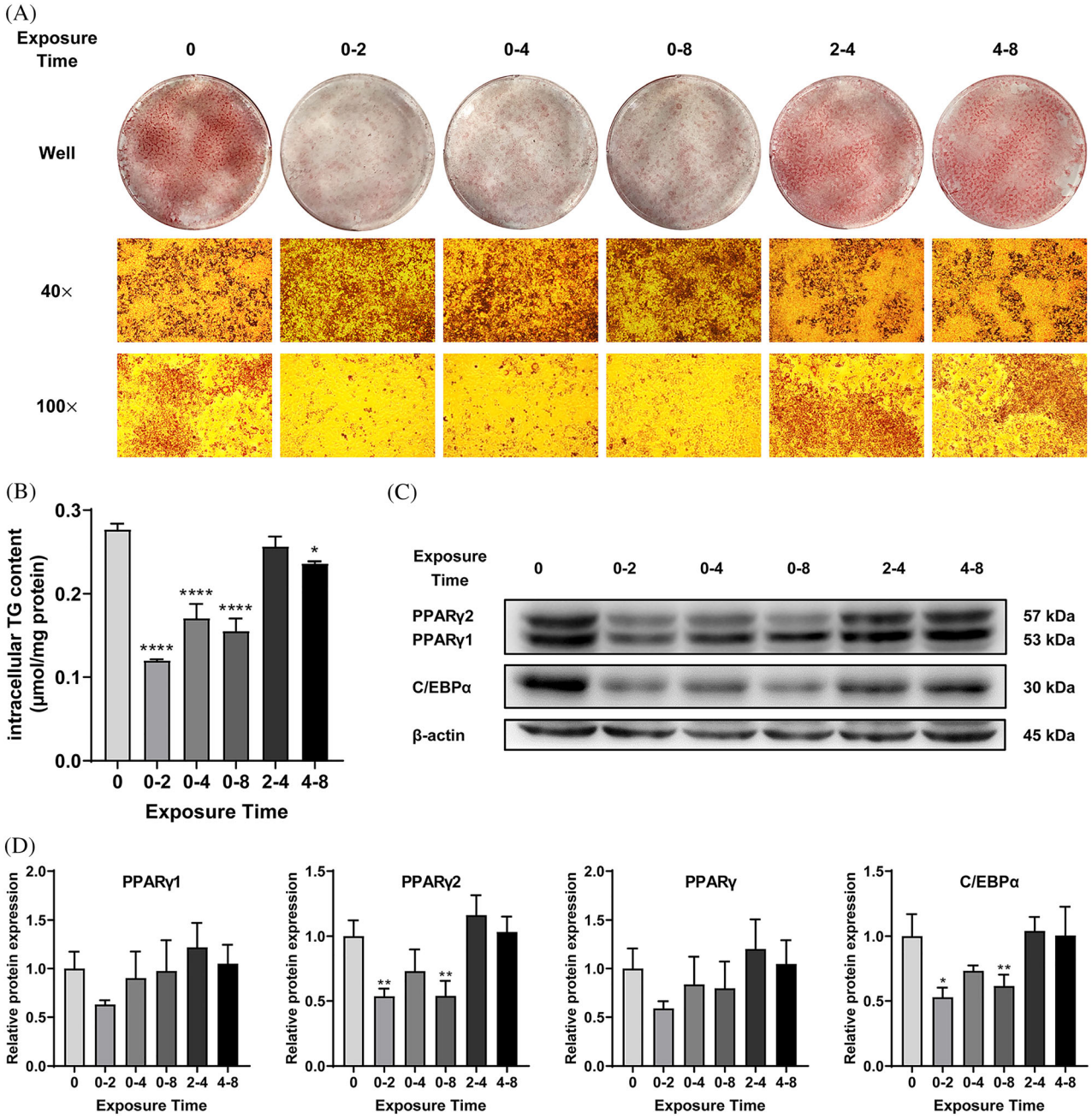

FIGURE 3 $La(NO_3)_3$ blocked the adipogenesis at the early stage of differentiation. The cells were differentiated by MDI medium and treated with 20 μM $La(NO_3)_3$ at different times. (A) The images of Oil Red O staining of the cells exposed to 20 μM $La(NO_3)_3$ at different days (Days 0–2, 0–4, 0–8, 2–4, and 4–8). (B) The intracellular TG contents in the cells treated with 20 μM $La(NO_3)_3$ at different days. (C) The protein expression levels of PPARγ1/2 and C/EBPα in the cells treated at different days. β-Actin was used as the loading protein. The protein bands were quantified using ImageJ software. (D) Relative protein expression levels of PPARγ1/2 and C/EBPα. The data are presented as the mean ± SD. $n = 3$. $^{*}p < 0.05$, $^{**}p < 0.01$, and $^{****}p < 0.0001$ compared to the control group.

phase to the S phase. Additionally, there were a significant reduction in the fraction of cells remaining at the G0/G1 phase and a concomitant increase in the G2/M phase (Table 3). Consistently, as shown in Figure 4D,E, the expression of CDK2, which played an important role in G1 to S checkpoint activation, was dose-dependently increased in the cells exposed to $La(NO_3)_3$. Also, by immunofluorescence staining, it was found that more cyclin D1 translocated to the cytosol in the $La(NO_3)_3$-treated cells at 20 h (Figure 4F).

3.5 | $La(NO_3)_3$ regulated transcription factors at the early phase of adipogenesis

At the early stage of adipogenesis, C/EBPβ acquires the ability of DNA binding and subsequently transactivates C/EBPα and PPARγ to promote adipogenesis. So we also examined the expression of related transcription factors. The results showed that after MDI induction for 48 h, the expression levels of C/EBPβ,

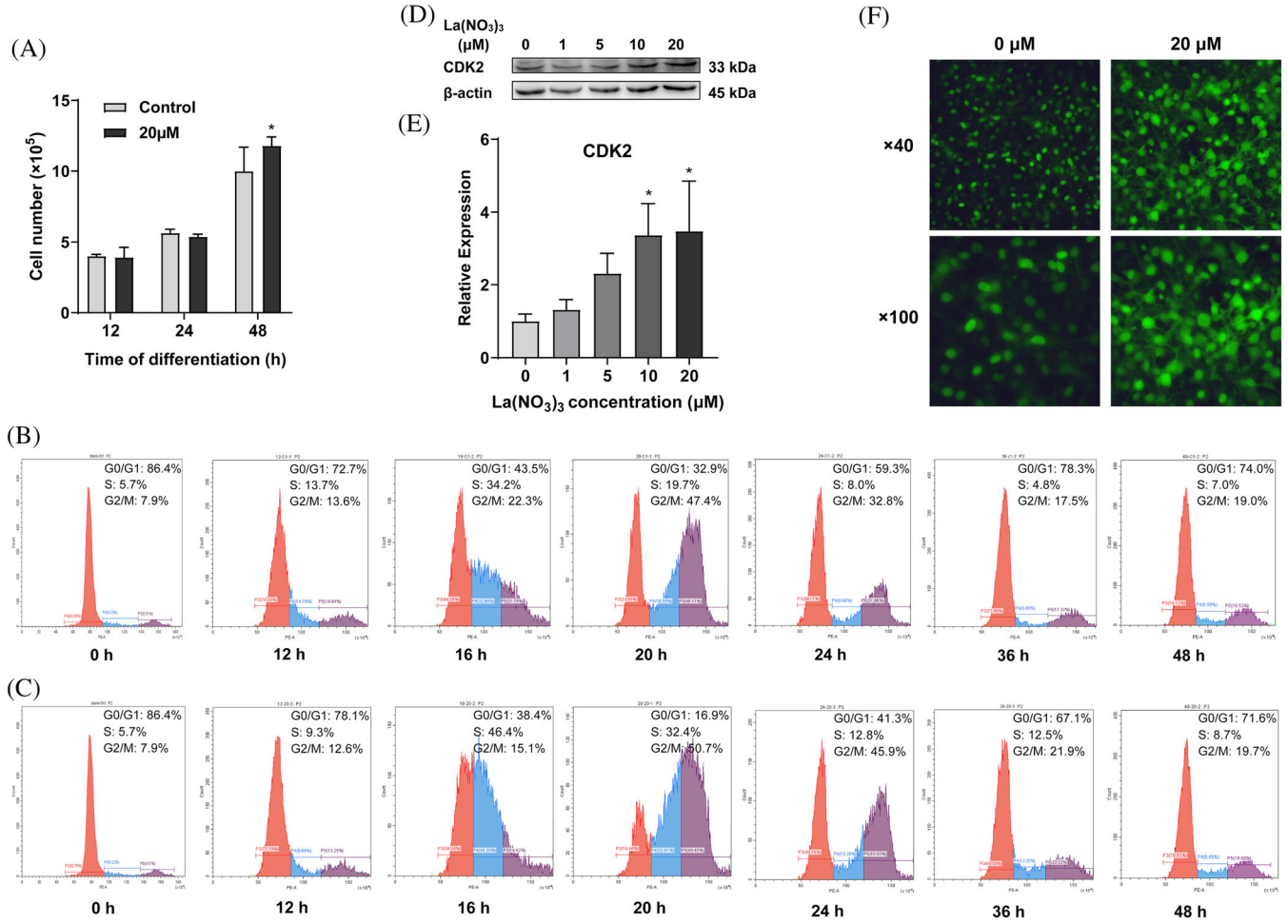

FIGURE 4 The effects of $La(NO_3)_3$ on cell proliferation and cell cycle progression during MCE. Post-confluent 3T3-L1 preadipocytes were induced to differentiate by MDI in the presence or absence of $La(NO_3)_3$. FACS analysis was performed during different times of the differentiation process. (A) The cellular viability of the differentiating preadipocytes treated with 20 μM $La(NO_3)_3$ for 12, 24, and 48 h was determined by the trypan blue assay. (B, C) Representative histograms and the distribution of the cell cycle in the cells treated without or with $La(NO_3)_3$, respectively. (D) The protein expression levels of CDK2 in the cells on Day 2. β-Actin was used as the loading protein. The protein bands were quantified using ImageJ software. (E) Relative protein expression levels of CDK2. (F) The immunofluorescence images of localization of cyclin D1 in the cells with or without $La(NO_3)_3$ treatment. The data are presented as the mean ± SD. $n = 3$. $^{*}p < 0.05$ compared to the control group.

TABLE 3 Effect of $La(NO_3)_3$ on cell cycle distribution at different time points during cell differentiation

	$La(NO_3)_3$ (μM)	0 h	12 h	16 h	20 h	24 h	36 h	48 h
%G0/G1	0	86.42 ± 0.33	72.69 ± 1.11	43.47 ± 1.77	32.95 ± 1.24	59.28 ± 0.67	78.27 ± 0.40	74.03 ± 0.94
	20		78.14 ± 1.47*	38.43 ± 2.56	16.90 ± 0.19****	41.35 ± 1.67***	67.07 ± 0.94*	71.56 ± 0.88
%S	0	5.71 ± 0.27	13.69 ± 1.75	34.20 ± 1.27	19.68 ± 0.04	7.95 ± 0.18	4.80 ± 0.43	7.01 ± 0.52
	20		9.26 ± 0.46	46.44 ± 1.51**	32.44 ± 1.83**	12.79 ± 0.60**	12.79 ± 0.60*	8.73 ± 0.30*
%G2/M	0	7.88 ± 0.06	13.62 ± 0.78	22.33 ± 0.50	47.38 ± 1.28	32.77 ± 0.85	17.48 ± 0.10	18.96 ± 0.42
	20		12.60 ± 1.44	15.13 ± 1.11**	50.66 ± 1.81	45.86 ± 1.49**	21.44 ± 1.03*	19.71 ± 1.15

Note: The results are presented as the mean ± SD.
$^{*}p < 0.05$. $^{**}p < 0.01$. $^{***}p < 0.001$. $^{****}p < 0.0001$ versus 0 μM compared to the control group.

C/EBPα, and PPARγ were significantly repressed by $La(NO_3)_3$ (Figure 5A,E).

As displayed in Figure 5B,C,F,G, $La(NO_3)_3$ induced a higher ratio of phosphorylated PI3K (pPI3K) and PI3K compared to the control, and the expression of Akt and the phosphorylation of PI3K were also slightly increased. Additionally, the ratio of phosphorylated STAT3 (pSTAT3) and STAT3 was significantly promoted at 48 h of MDI induction in the $La(NO_3)_3$-treated cells (Figure 5D,H). These results indicated that STAT3 and PI3K might be involved in the $La(NO_3)_3$-induced disorders of the MCE process of 3T3-L1 preadipocytes.

3.6 | $La(NO_3)_3$ enhanced the canonical wnt signaling pathway and increased nuclear translocation of β-catenin

To further investigate the underlying mechanism of the adipogenesis inhibition of $La(NO_3)_3$, the canonical wnt signaling pathway was investigated. The results showed that the protein expression levels of β-catenin significantly increased in $La(NO_3)_3$-treated cells on Day 8 (Figure 6A,B). As Figure 6A showed, the treatment of $La(NO_3)_3$ also induced a higher level of cyclin D1 in the differentiating cells on Day 8. However, $La(NO_3)_3$ did not enhance the expression of

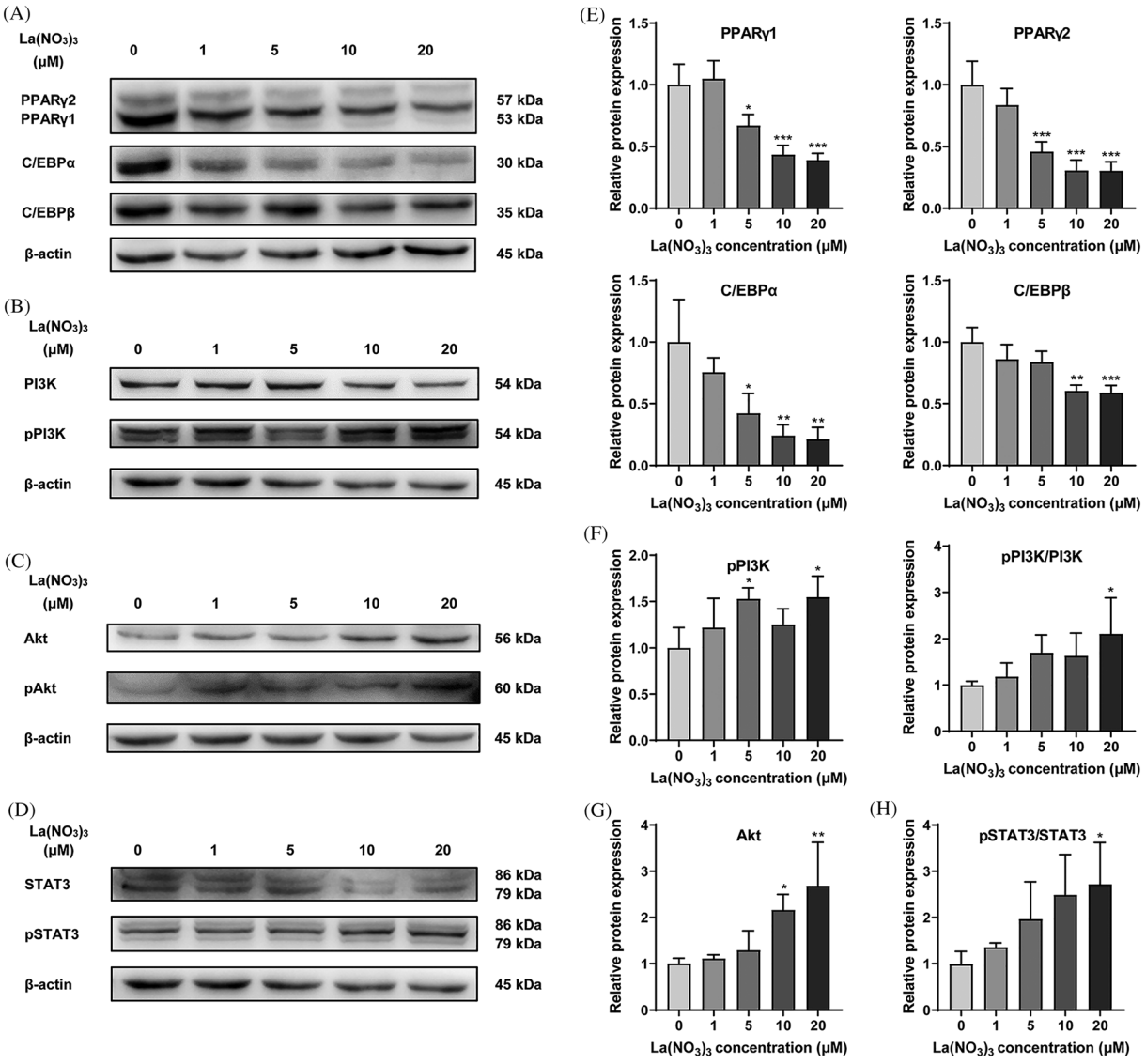

FIGURE 5 $La(NO_3)_3$ regulated transcription factors at the early phase of adipogenesis. 3T3-L1 preadipocytes were induced to differentiate by MDI in the presence or absence of $La(NO_3)_3$ for 2 days. (A) The protein expression levels of C/EBPβ, C/EBPα, and PPARγ in the cells treated with different concentrations of $La(NO_3)_3$. (B) The protein expression levels of PI3K and pPI3K. (C) The protein expression levels of Akt and pAkt. (D) The protein expression levels of STAT3 and pSTAT3. (E) Relative protein expression levels of C/EBPβ, C/EBPα, and PPARγ. (F) Relative protein expression levels of PI3K and pPI3K. (G) Relative protein expression level of Akt. (H) The ratio of the relative protein expression levels of STAT3 and pSTAT3. β-Actin was used as the loading protein. The protein bands were quantified using ImageJ software. The data are presented as the mean ± SD. $n = 3$. $^{*}p < 0.05$, $^{**}p < 0.01$, and $^{***}p < 0.001$ compared to the control group.

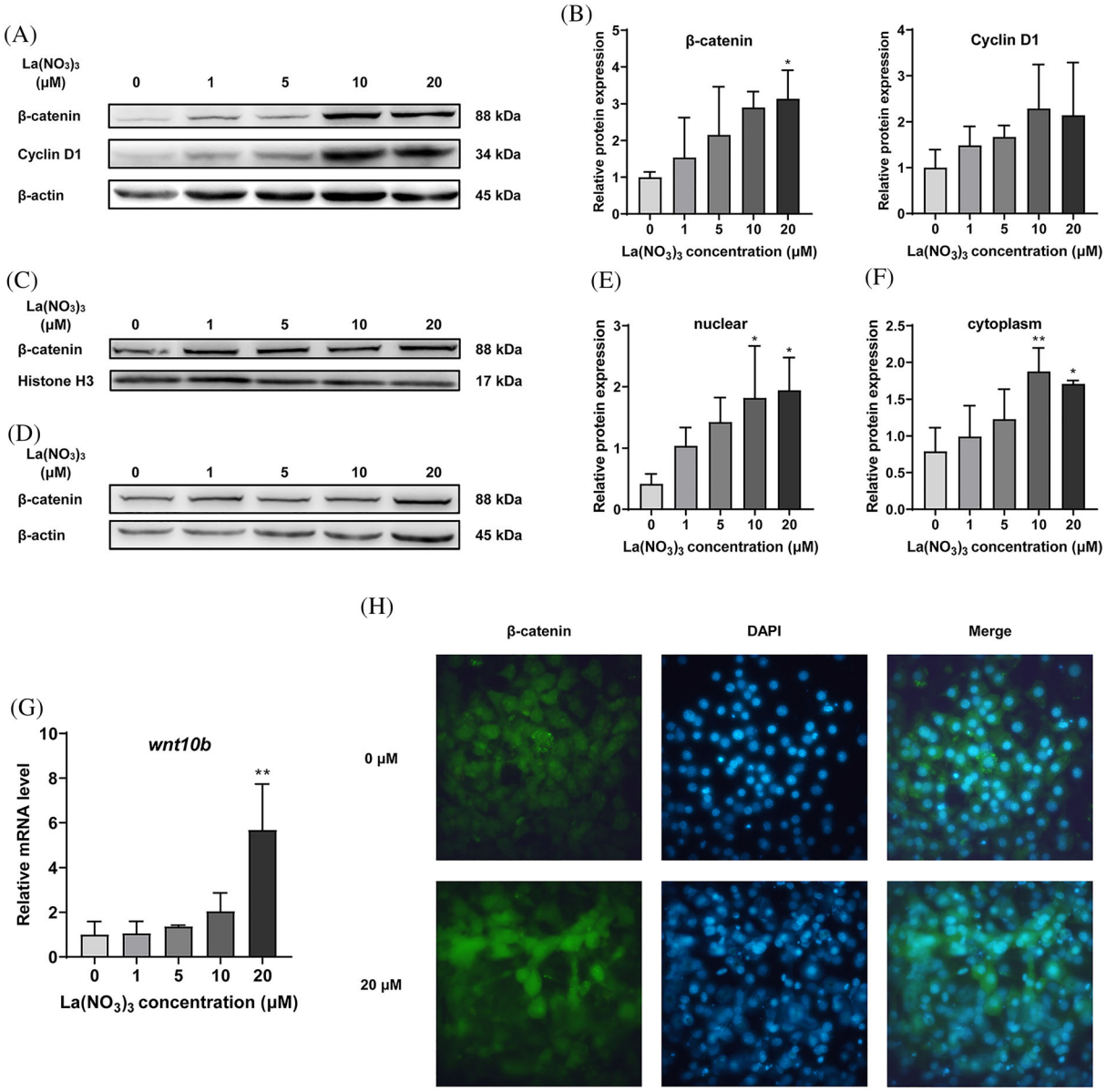

FIGURE 6 $La(NO_3)_3$ enhanced the canonical wnt signaling pathway and increased nuclear translocation of β-catenin. (A) The protein expression level of β-catenin and cyclin D1 in the cells treated with different concentrations of $La(NO_3)_3$ on Day 8. (B) Relative protein expression levels of β-catenin. (C) The protein expression level of nuclear β-catenin. Histone H3 was used as the loading protein. (D) The protein expression level of cytoplasm β-catenin. β-Actin was used as the loading protein. The protein bands were quantified using ImageJ software. (E) Relative protein expression levels of nuclear β-catenin. (F) Relative protein expression levels of cytoplasm β-catenin. (G) The mRNA expression levels of *wnt10b*. The relative mRNA expression levels were calculated using $2^{-\Delta\Delta Ct}$ method. (H) The immunofluorescence images of localization of β-catenin relative to nucleus (DAPI stained) with or without $La(NO_3)_3$ treatment. The magnification is 100×. The data are presented as the mean ± SD. $n = 3$. $^{*}p < 0.05$ and $^{**}p < 0.01$ compared to the control group.

β-catenin in the differentiating cells on Day 2 (data not shown), which suggested that the canonical wnt pathway was triggered after MCE. Furthermore, the treatment of $La(NO_3)_3$ did promote the expression of β-catenin in the nuclear, and β-catenin expression in the cytoplasm also increased (Figure 6C–F). Immunofluorescence and DAPI nuclear staining also proved that $La(NO_3)_3$ induced the nuclear translocation of β-catenin (Figure 6H). Additionally, as shown in Figure 6G, the mRNA expression level of *wnt10b*, which is one of the anti-adipogenic wnt signals, was elevated in the cells exposed to $La(NO_3)_3$.

4 | DISCUSSION

As one of the largest endocrine organs in the body, adipose tissue plays a pivotal role in energy and glycolipid metabolism through secreting various adipokines and is involved in many signaling pathways (Poulos et al., 2010). The appropriate changes in adipose tissue could modulate the body to adapt to the various internal and external challenges, but both the excess and deficiency of adipose tissue would result in metabolic disorders and other adverse health effects.

Several studies have reported that lanthanides might influence glycolipid metabolism in vivo and inhibit adipogenesis in some in vitro cell models. In this study, we observed the inhibitory effect of $La(NO_3)_3$ on the adipogenic differentiation of 3T3-L1 preadipocytes and explored its underlying mechanisms. The results demonstrated that $La(NO_3)_3$ mainly performed a suppression on adipogenesis during the early stage of the differentiation process, and the canonical wnt signaling pathway might be involved in it. Furthermore, it was found that $La(NO_3)_3$ could promote the cell proliferation of 3T3-L1 preadipocytes before MDI induction and disorder the cell cycle progression during MCE after stimulation.

The mouse embryonic fibroblast cell line 3T3-L1 is one of the most used in vitro models of adipocyte differentiation. Contact inhibition prior to the differentiation is required for 3T3-L1 preadipocytes to continue the following differentiation into adipocytes (Chang & Polakis, 1978). In the present study, it was shown that $La(NO_3)_3$ could promote cell growth after treatment for 48 h (Figure 1A). Similarly, several studies have shown that exposure to the lanthanides ($LaCl_3$, $CeCl_3$, and $GdCl_3$) resulted in a significant increase in cell growth of 3T3-L1 preadipocytes, and $GdCl_3$ could also exert the proliferation-promoting effect on NIH 3T3 cells (He et al., 2006; Hou et al., 2013; Smith & Smith, 1984). Some researchers speculated that the promotion of cell proliferation might be due to the transmembrane fluxes of Ca^{2+} whose binding sites could be taken up by La^{3+} or Ce^{3+} (He et al., 2006; Segal, 1986).

After the addition of MDI, 3T3-L1 preadipocytes begin to differentiate towards adipocytes and eventually acquire adipocyte characteristics. The formation of intracellular lipid droplets is one of the characteristics of adipogenic differentiation. In this study, the results of Oil Red O staining and intracellular TG content suggested that $La(NO_3)_3$ could significantly inhibit the adipogenesis process (Figure 2A,B). C/EBPα and PPARγ are key transcriptional factors of adipogenesis that induce the synthesis of TG and activate the expression of target genes, including LPL and Leptin (Moseti et al., 2016). The downregulated expression levels of *lpl* mRNA, PPARγ, and C/EBPα, especially PPARγ2, which is predominantly highly expressed in adipocytes, also confirmed that $La(NO_3)_3$ inhibited adipogenic differentiation in 3T3-L1 preadipocytes (Figure 2C–F). Studies have shown that 3T3-L1 preadipocytes have several specific differentiation stages. In this study, we further analyzed the main effect stage of $La(NO_3)_3$. Oil Red O staining, TG content, and the reduced expressions of C/EBPα and PPARγ in the cells treated with $La(NO_3)_3$ at different times during the differentiation process all showed that $La(NO_3)_3$ inhibited the adipogenesis mainly on Days 0–2 (Figure 3). Considering that 3T3-L1 preadipocytes re-enter the cell cycle and undergo the MCE process during the first 2 days, the results suggested that $La(NO_3)_3$ might disorder the MCE process of 3T3-L1 preadipocytes to inhibit terminal adipogenic differentiation.

After growth arrest at confluence, preadipocytes receive appropriate signals to enter MCE for about two rounds of division (Gregoire et al., 1998). Our current data exhibited a disorder of MCE in $La(NO_3)_3$-treated cells, which was evidenced by a higher growth rate than the control cells after MDI stimulation, an increase in S and G2/M populations, and a decrease in G0/G1 populations (Figure 4A–C and Table 3). The cell cycle process is regulated by a variety of cyclin-dependent kinases (CDKs) and other related proteins, such as CDK2, CDK4, CDK6, cyclin D1, and Rb. Upon confluence, preadipocytes are arrested in the G0/G1 phase with low expression of cyclin D1, and MDI stimulation induces the synthesis of cyclin D1, which leads to the formation of cyclin D–CDK4/6 complex and subsequently the activation of CDK2/cyclin E (Chang & Kim, 2019; Łukasik et al., 2021; Suzuki et al., 2000). Activated CDK2 and CDK4/6, which are important cell cycle components involved in the transition from the G1 to the S phase, could phosphorylate Rb resulting in the release of the transcription factor E2F. The facilitated expressions of E2F target genes are also required for DNA synthesis and the S-phase entry (Farmer, 2006; Sherr & McCormick, 2002). Additionally, cyclin D1 accumulates from the G1 phase and translocates from the nucleus to the cytoplasm at the S phase (Alao, 2007; Baldin et al., 1993). The elevated protein expression of CDK2 and distribution of cyclin D1 in the cytoplasm indicated that $La(NO_3)_3$ promoted the S-phase entry (Figure 4D–F). It was reported that the PI3K/Akt pathway regulated the expressions of cyclin D and p27 to modulate the cell cycle progression and the phosphorylation of STAT3 during the proliferation phase of adipogenesis stimulated the cell growth (Cernkovich et al., 2007; Xu & Liao, 2004). The increased expression of Akt and the higher phosphorylation level of PI3K and STAT3 in $La(NO_3)_3$-treated cells suggested that $La(NO_3)_3$ might also activate the PI3K/Akt and STAT3 to promote cell proliferation during MCE (Figure 5B–H).

3T3-L1 preadipocytes exit the cell cycle for terminal differentiation after several rounds of DNA synthesis (Tang et al., 2003). Several studies have shown that the inhibition of adipogenesis in 3T3-L1 preadipocytes could result from the delayed entry of G0/G1 cells to the S phase, instead of the promotion of the S-phase entry (Jang et al., 2017; Lee et al., 2020). It was reported that $GdCl_3$, which is also one kind of lanthanides, was able to promote cell cycle entry into the S phase but inhibit adipogenesis of 3T3-L1 preadipocytes due to the sustained extracellular signal-regulated kinase (ERK) activation and pro-proliferation ability throughout the whole differentiation (Hou et al., 2013). The expression of ERK was also detected in this study, but there was no statistical change in $La(NO_3)_3$-treated cells (data not shown). In this study, it was shown that there were fewer cells remaining in the G0/G1 phase at 36 and 48 h, but more cells existed in the S phase under $La(NO_3)_3$ treatment (Table 3). Therefore, we hypothesized that $La(NO_3)_3$ might block the cell cycle exit leading to more cells remaining in the mitosis process. C/EBPα and PPARγ are concerned to be antimitotic and could control the withdrawal of preadipocytes from the cell cycle during terminal differentiation, and C/EBPα is activated when MCE ceases (Shao & Lazar, 1997; Tang & Lane, 1999). Our data showed that the expressions of C/EBPα and PPARγ were significantly downregulated at 48 h of differentiation in the $La(NO_3)_3$-treated cells, which indicated the impaired cell cycle exit and continued MCE process (Figure 5A,E). Besides, C/EBPβ, the early transcription factor that induces PPARγ and C/EBPα, was also

downregulated in $La(NO_3)_3$-treated cells (Figure 5A,E), which might also partly explain the inhibitory effect of $La(NO_3)_3$ on adipogenesis at the early stage of differentiation. Furthermore, studies have shown that CDK2 could phosphorylate and activate C/EBPβ (Li et al., 2007), but in our study, the expression of C/EBPβ was downregulated in the $La(NO_3)_3$-treated cells, which suggested that $La(NO_3)_3$ might downregulate C/EBPβ directly or through other cell cycle-related regulators. In combination, $La(NO_3)_3$ could result in the cells arrested in the mitosis process, cell retention then, and failure for terminal differentiation.

It has been shown that the inhibition of adipogenesis is often accompanied by cell cycle arrest. Wang et al. (2020) found that 3T3-L1 preadipocytes treated with lactucin failed to undergo MCE due to reduced phosphorylation of Janus kinase 2 (JAK2) and STAT3 and were also inhibited for adipogenesis. On the other hand, there are still some studies with different results. Hashimoto et al. (2019) found that phorbol 12-myristate 13-acetate suppressed adipocyte differentiation but enhance the proliferation of bone marrow stromal cells (BMSCs). A study about DNA (cytosine-5)-methyltransferase 3A also indicated that methylation of PPARγ promoter could decrease lipid accumulation, and methylation of p21 promoter promoted cell proliferation in porcine intramuscular preadipocytes (Qimuge et al., 2019). Cell proliferation and differentiation are closely related during adipogenesis, and many regulating factors interact in both processes (Fajas, 2003). The specific relationship between cell proliferation and differentiation and the mechanisms about it are not yet clear; thus, more research is needed to explore the relationship, which could help to more fully understand how $La(NO_3)_3$ and other lanthanides affect cell proliferation and adipogenesis.

Adipogenesis is regulated by several highly conserved signaling pathways, among which the canonical wnt/β-catenin pathway exerts an anti-adipogenic effect (Rosen & MacDougald, 2006). Wnt10b is an anti-adipogenic wnt signal participating in the canonical wnt pathway. Wnt10b binds to frizzled receptors and LRP5/6 co-receptors and inactivates the degradation complex acting on β-catenin. Hypophosphorylated β-catenin then translocates to the nucleus leading to the activation of target genes and the suppression of C/EBPα and PPARγ (Christodoulides et al., 2009). The treatment of $La(NO_3)_3$ on Days 4–8 also showed a modest suppression of the adipogenic differentiation, which indicated that $La(NO_3)_3$ might exert its inhibitory effect on adipogenesis through other mechanisms. Therefore, we investigated the canonical wnt pathway to further elucidate the mechanisms involved. Our data revealed that $La(NO_3)_3$ increased the expressions of *wnt10b* and β-catenin significantly in 3T3-L1 preadipocytes and the nucleus distribution of β-catenin also increased in $La(NO_3)_3$-treated cells on Day 8 (Figure 6). Also, the expression levels of C/EBPα and PPARγ were reduced significantly in $La(NO_3)_3$-treated cells on Day 8. These results suggested that $La(NO_3)_3$ could inhibit key transcription factors C/EBPα and PPARγ during the terminal differentiation stage of 3T3-L1 preadipocytes by promoting the canonical wnt pathway and the nuclear translocation of β-catenin, thereby suppressing adipogenesis. We also found that the expressions of LRP5/6 were not changed (data not shown), suggesting that $La(NO_3)_3$ might enhance the wnt10b signal without increasing the LRP5/6 receptors on 3T3-L1 preadipocytes. In addition, β-catenin can interact with transcription factors after translocating to the nuclear and upregulate cyclin D1 then. Cyclin D1 is related to the regulation of the cell cycle and cellular proliferation and can repress PPARγ function to inhibit adipogenesis (Fu et al., 2005). Consistently, our results showed an increase in the expression of cyclin D1 and a reduction of the expression of PPARγ in $La(NO_3)_3$-treated cells in the terminal differentiation stage (Figure 6A,B), from which we could associate the effect of $La(NO_3)_3$ on the wnt signaling pathway with the upregulation of cyclin D1 and suppression of PPARγ partly.

5 | CONCLUSION

Our results demonstrated that $La(NO_3)_3$ inhibited adipogenesis in 3T3-L1 preadipocytes. The anti-adipogenic effect of $La(NO_3)_3$ was mainly exerted during the early stage of the differentiation process, and the wnt/β-catenin signaling pathway might be involved in it. Furthermore, $La(NO_3)_3$ influenced the S-phase entry and the withdrawal from the cell cycle during the MCE process. Additionally, $La(NO_3)_3$ also enhanced cell proliferation of 3T3-L1 preadipocytes without MDI stimulation. Further in vivo studies are needed to verify the anti-adipogenic effect of $La(NO_3)_3$, which can provide more evidence for the effect of $La(NO_3)_3$ on glucose and lipid metabolism and human health.

ACKNOWLEDGEMENT

The authors are grateful for the financial support by National Key Research and Development Program of China (Grant No. 2017YFC1600203).

CONFLICTS OF INTEREST

The authors declare that there are no conflicts of interest.

ORCID

Xuetao Wei https://orcid.org/0000-0001-5902-9973
Weidong Hao https://orcid.org/0000-0001-5879-450X

REFERENCES

Alao, J. P. (2007). The regulation of cyclin D1 degradation: Roles in cancer development and the potential for therapeutic invention. *Molecular Cancer*, *6*, 24. https://doi.org/10.1186/1476-4598-6-24

Ali, A. T., Hochfeld, W. E., Myburgh, R., & Pepper, M. S. (2013). Adipocyte and adipogenesis. *European Journal of Cell Biology*, *92*(6–7), 229–236. https://doi.org/10.1016/j.ejcb.2013.06.001

Baldin, V., Lukas, J., Marcote, M. J., Pagano, M., & Draetta, G. (1993). Cyclin D1 is a nuclear protein required for cell cycle progression in G1. *Genes & Development*, *7*(5), 812–821. https://doi.org/10.1101/gad.7.5.812

Capeau, J., Magré, J., Lascols, O., Caron, M., Béréziat, V., Vigouroux, C., & Bastard, J. P. (2005). Diseases of adipose tissue: Genetic and acquired lipodystrophies. *Biochemical Society Transactions*, *33*(Pt 5), 1073–1077. https://doi.org/10.1042/bst0331073

Cernkovich, E. R., Deng, J., Hua, K., & Harp, J. B. (2007). Midkine is an autocrine activator of signal transducer and activator of transcription

3 in 3T3-L1 cells. *Endocrinology*, *148*(4), 1598–1604. https://doi.org/10.1210/en.2006-1106

Chang, E., & Kim, C. Y. (2019). Natural products and obesity: A focus on the regulation of mitotic clonal expansion during adipogenesis. *Molecules*, *24*(6), 1157. https://doi.org/10.3390/molecules24061157

Chang, T. H., & Polakis, S. E. (1978). Differentiation of 3T3-L1 fibroblasts to adipocytes. Effect of insulin and indomethacin on the levels of insulin receptors. *The Journal of Biological Chemistry*, *253*(13), 4693–4696. https://doi.org/10.1016/S0021-9258(17)30445-3

Chen, D., Liu, Y., Chen, A. J., & Nie, Y. X. (2003). Experimental study of subchronic toxicity of lanthanum nitrate on liver in rats. *Nonlinearity in Biology Toxicology and Medicine*, *1*(4), 469–480. https://doi.org/10.1080/15401420390271074

Cheng, J., Cheng, Z., Hu, R., Cui, Y., Cai, J., Li, N., Gui, S., Sang, X., Sun, Q., Wang, L., & Hong, F. (2014). Immune dysfunction and liver damage of mice following exposure to lanthanoids. *Environmental Toxicology*, *29*(1), 64–73. https://doi.org/10.1002/tox.20773

Christodoulides, C., Lagathu, C., Sethi, J. K., & Vidal-Puig, A. (2009). Adipogenesis and WNT signalling. *Trends in Endocrinology and Metabolism*, *20*(1), 16–24. https://doi.org/10.1016/j.tem.2008.09.002

Fajas, L. (2003). Adipogenesis: A cross-talk between cell proliferation and cell differentiation. *Annals of Medicine*, *35*(2), 79–85. https://doi.org/10.1080/07853890310009999

Farmer, S. R. (2006). Transcriptional control of adipocyte formation. *Cell Metabolism*, *4*(4), 263–273. https://doi.org/10.1016/j.cmet.2006.07.001

Fu, M., Rao, M., Bouras, T., Wang, C., Wu, K., Zhang, X., Li, Z., Yao, T. P., & Pestell, R. G. (2005). Cyclin D1 inhibits peroxisome proliferator-activated receptor γ-mediated adipogenesis through histone deacetylase recruitment. *Journal of Biological Chemistry*, *280*(17), 16934–16941. https://doi.org/10.1074/jbc.M500403200

Galic, S., Oakhill, J. S., & Steinberg, G. R. (2010). Adipose tissue as an endocrine organ. *Molecular and Cellular Endocrinology*, *316*(2), 129–139. https://doi.org/10.1016/j.mce.2009.08.018

Gregoire, F. M., Smas, C. M., & Sul, H. S. (1998). Understanding adipocyte differentiation. *Physiological Reviews*, *78*(3), 783–809. https://doi.org/10.1152/physrev.1998.78.3.783

Grosjean, N., Le Jean, M., Berthelot, C., Chalot, M., Gross, E. M., & Blaudez, D. (2019). Accumulation and fractionation of rare earth elements are conserved traits in the *Phytolacca* genus. *Scientific Reports*, *9*(1), 18458. https://doi.org/10.1038/s41598-019-54238-3

Han, G., Tan, Z., Jing, H., Ning, J., Li, Z., Gao, S., & Li, G. (2021). Comet assay evaluation of lanthanum nitrate DNA damage in C57-ras transgenic mice. *Biological Trace Element Research*, *199*(10), 3728–3736. https://doi.org/10.1007/s12011-020-02500-5

Hashimoto, R., Miyamoto, Y., Itoh, S., Daida, H., Okada, T., & Katoh, Y. (2019). Phorbol 12-myristate 13-acetate (PMA) suppresses high Ca^{2+}-enhanced adipogenesis in bone marrow stromal cells. *Journal of Physiological Sciences*, *69*(5), 741–748. https://doi.org/10.1007/s12576-019-00690-9

He, M. L., Yang, W. Z., Hidari, H., & Rambeck, W. A. (2006). Effect of rare earth elements on proliferation and fatty acids accumulation of 3T3-L1 cells. *Asian-Australasian Journal of Animal Sciences*, *19*(1), 119–125. https://doi.org/10.5713/ajas.2006.119

Hou, C. C., Feng, M., Wang, K., & Yang, X. G. (2013). Lanthanides inhibit adipogenesis with promotion of cell proliferation in 3T3-L1 preadipocytes. *Metallomics*, *5*(6), 715–722. https://doi.org/10.1039/c3mt00020f

Jang, M. K., Yun, Y. R., Kim, J. H., Park, M. H., & Jung, M. H. (2017). Gomisin N inhibits adipogenesis and prevents high-fat diet-induced obesity. *Scientific Reports*, *7*, 40345. https://doi.org/10.1038/srep40345

Kawai, T., Autieri, M. V., & Scalia, R. (2021). Adipose tissue inflammation and metabolic dysfunction in obesity. *American Journal of Physiology-Cell Physiology*, *320*(3), C375–c391. https://doi.org/10.1152/ajpcell.00379.2020

Lee, Y. S., Park, J. S., Lee, D. H., Han, J., & Bae, S. H. (2020). Ezetimibe ameliorates lipid accumulation during adipogenesis by regulating the AMPK–mTORC1 pathway. *FASEB Journal*, *34*(1), 898–911. https://doi.org/10.1096/fj.201901569R

Lefterova, M. I., & Lazar, M. A. (2009). New developments in adipogenesis. *Trends in Endocrinology and Metabolism*, *20*(3), 107–114. https://doi.org/10.1016/j.tem.2008.11.005

Leow, M. K., Addy, C. L., & Mantzoros, C. S. (2003). Clinical review 159: Human immunodeficiency virus/highly active antiretroviral therapy-associated metabolic syndrome: Clinical presentation, pathophysiology, and therapeutic strategies. *The Journal of Clinical Endocrinology and Metabolism*, *88*(5), 1961–1976. https://doi.org/10.1210/jc.2002-021704

Li, R., Zhou, Y., Liu, W., Li, Y., Qin, Y., Yu, L., Chen, Y., & Xu, Y. (2021). Rare earth element lanthanum protects against atherosclerosis induced by high-fat diet via down-regulating MAPK and NF-κB pathways. *Ecotoxicology and Environmental Safety*, *207*, 111195. https://doi.org/10.1016/j.ecoenv.2020.111195

Li, X., Kim, J. W., Grønborg, M., Urlaub, H., Lane, M. D., & Tang, Q. Q. (2007). Role of cdk2 in the sequential phosphorylation/activation of C/EBPβ during adipocyte differentiation. *Proceedings of the National Academy of Sciences of the United States of America*, *104*(28), 11597–11602. https://doi.org/10.1073/pnas.0703771104

Liu, D., Ge, K., Sun, J., Chen, S., Jia, G., & Zhang, J. (2015). Lanthanum breaks the balance between osteogenesis and adipogenesis of mesenchymal stem cells through phosphorylation of Smad1/5/8. *RSC Advances*, *5*(53), 42233–42241. https://doi.org/10.1039/C5RA02311D

Longo, K. A., Wright, W. S., Kang, S., Gerin, I., Chiang, S. H., Lucas, P. C., Opp, M. R., & MacDougald, O. A. (2004). Wnt10b inhibits development of white and brown adipose tissues. *Journal of Biological Chemistry*, *279*(34), 35503–35509. https://doi.org/10.1074/jbc.M402937200

Łukasik, P., Załuski, M., & Gutowska, I. (2021). Cyclin-dependent kinases (CDK) and their role in diseases development—Review. *International Journal of Molecular Sciences*, *22*(6), 2935. https://doi.org/10.3390/ijms22062935

McGown, C., Birerdinc, A., & Younossi, Z. M. (2014). Adipose tissue as an endocrine organ. *Clinical Liver Disease*, *18*(1), 41–58. https://doi.org/10.1016/j.cld.2013.09.012

Moseti, D., Regassa, A., & Kim, W. K. (2016). Molecular regulation of adipogenesis and potential anti-adipogenic bioactive molecules. *International Journal of Molecular Sciences*, *17*(1), 124. https://doi.org/10.3390/ijms17010124

Poulos, S. P., Hausman, D. B., & Hausman, G. J. (2010). The development and endocrine functions of adipose tissue. *Molecular and Cellular Endocrinology*, *323*(1), 20–34. https://doi.org/10.1016/j.mce.2009.12.011

Qimuge, N., He, Z., Qin, J., Sun, Y., Wang, X., Yu, T., Dong, W., Yang, G., & Pang, W. (2019). Overexpression of DNMT3A promotes proliferation and inhibits differentiation of porcine intramuscular preadipocytes by methylating p21 and PPARg promoters. *Gene*, *696*, 54–62. https://doi.org/10.1016/j.gene.2019.02.029

Rosen, E. D., & MacDougald, O. A. (2006). Adipocyte differentiation from the inside out. *Nature Reviews Molecular Cell Biology*, *7*(12), 885–896. https://doi.org/10.1038/nrm2066

Sarjeant, K., & Stephens, J. M. (2012). Adipogenesis. *Cold Spring Harbor Perspectives in Biology*, *4*(9), a008417. https://doi.org/10.1101/cshperspect.a008417

Segal, J. (1986). Lanthanum increases the rat thymocyte cytoplasmic free calcium concentration by enhancing calcium influx. *Biochimica et Biophysica Acta*, *886*(2), 267–271. https://doi.org/10.1016/0167-4889(86)90144-8

Shao, D., & Lazar, M. A. (1997). Peroxisome proliferator activated receptor γ, CCAAT/enhancer-binding protein α, and cell cycle status regulate

the commitment to adipocyte differentiation. *Journal of Biological Chemistry*, *272*(34), 21473–21478. https://doi.org/10.1074/jbc.272.34.21473

Sherr, C. J., & McCormick, F. (2002). The RB and p53 pathways in cancer. *Cancer Cell*, *2*(2), 103–112. https://doi.org/10.1016/s1535-6108(02)00102-2

Smith, J. B., & Smith, L. (1984). Initiation of DNA synthesis in quiescent Swiss 3T3 and 3T6 cells by lanthanum. *Bioscience Reports*, *4*(9), 777–782. https://doi.org/10.1007/bf01128819

Suzuki, A., Hayashida, M., Ito, T., Kawano, H., Nakano, T., Miura, M., Akahane, K., & Shiraki, K. (2000). Survivin initiates cell cycle entry by the competitive interaction with Cdk4/p16^{INK4a} and Cdk2/cyclin E complex activation. *Oncogene*, *19*(29), 3225–3234. https://doi.org/10.1038/sj.onc.1203665

Tang, Q. Q., & Lane, M. D. (1999). Activation and centromeric localization of CCAAT/enhancer-binding proteins during the mitotic clonal expansion of adipocyte differentiation. *Genes & Development*, *13*(17), 2231–2241. https://doi.org/10.1101/gad.13.17.2231

Tang, Q. Q., Otto, T. C., & Lane, M. D. (2003). Mitotic clonal expansion: A synchronous process required for adipogenesis. *Proceedings of the National Academy of Sciences of the United States of America*, *100*(1), 44–49. https://doi.org/10.1073/pnas.0137044100

Wang, X., Liu, M., Cai, G. H., Chen, Y., Shi, X. C., Zhang, C. C., Xia, B., Xie, B. C., Liu, H., Zhang, R. X., Lu, J. F., Zhu, M. Q., Yang, S. Z., Chu, X. Y., Zhang, D. Y., Wang, Y. L., & Wu, J. W. (2020). A potential nutraceutical candidate lactucin inhibits adipogenesis through downregulation of JAK2/STAT3 signaling pathway-mediated mitotic clonal expansion. *Cell*, *9*(2), 331. https://doi.org/10.3390/cells9020331

Xu, J., & Liao, K. (2004). Protein kinase B/AKT 1 plays a pivotal role in insulin-like growth factor-1 receptor signaling induced 3T3-L1 adipocyte differentiation. *Journal of Biological Chemistry*, *279*(34), 35914–35922. https://doi.org/10.1074/jbc.M402297200

Zhang, J., Li, Y., Zhang, Q., Hao, X., & Wang, S. (2012). Effects of gadolinium on proliferation, differentiation and calcification of primary mouse osteoblasts in vitro. *Journal of Rare Earths*, *30*(8), 831–834. https://doi.org/10.1016/S1002-0721(12)60139-2

How to cite this article: Xu, L., Xiao, Q., Kang, C., Wei, X., & Hao, W. (2022). Lanthanum nitrate inhibits adipogenesis in 3T3-L1 preadipocytes with a disorder of mitotic clonal expansion process. *Journal of Applied Toxicology*, 1–14. https://doi.org/10.1002/jat.4391